

**A computational approach to identify novel inhibitor for the drug resistant
Mycobacterium tuberculosis DprE1 enzyme**

Chaitali Dhande^{1‡}, Devanshi Mistry^{2‡}, Anandakrishnan Karthic^{3‡}, Rajshri Singh^{3,4}, Sagar Barage^{3,5*}

Email: tejaswinid@gmail.com, devanshibmistry@gmail.com, karthic28199@gmail.com, rsingh1@mum.amity.edu, sagarbarage@gmail.com

¹School of Biotechnology and Bioinformatics, D.Y. Patil University, CBD Belapur, Navi Mumbai – 400614, Maharashtra, India

²Institute of Chemical Technology (ICT), Mumbai - 400019, Maharashtra, India

³Amity Institute of Biotechnology, Amity University, Mumbai - Pune Expressway, Bhatan, Post-Somathne, Panvel - 410206, Maharashtra, India.

⁴Centre for Proteomics and Drug Discovery, Amity University, Mumbai - Pune Expressway, Bhatan, Post-Somathne, Panvel - 410206, Maharashtra, India.

⁵Centre for Computational Biology and Translational Research, Amity University, Mumbai - Pune Expressway, Bhatan, Post-Somathne, Panvel - 410206, Maharashtra, India.

Supplementary Material

FASTA Entry of P9WJF0

```
>sp|P9WJF0|DPRE1_MYCTO      Decaprenylphosphoryl-beta-D-ribose      oxidase
OS=Mycobacterium tuberculosis (strain CDC 1551 / Oshkosh) OX=83331 GN=dprE1 PE=3
SV=1
MLSVGATTTATRLTGWGRTAPSVANVLRTPDAEMIVKAVARVAESGGGRGAIARG
LGRSYGDNAQNGGGLVIDMTPLNTIHSIDADTKLVDIDAGVNLDQLMKAALPFGLW
VPVLPGTRQVTVGGAIACDIHGKNHHSAGSFGNHVRSMDLLTADGEIRHLTPTGEDA
ELFWATVGGNGLTGIIMRATIEMTPTSTAYFIADGDVTASLDETIALHSDGSEARYTY
SSAWFDAISAPPKLGRAAVSRGRLATVEQLPAKLRSEPLKFDAPQLLTPDVFVFNGLA
NKYTFGPIGELWYRKSGTYRGKVQNLTKQFYHPLDMFGEWNRAYGPAGFLQYQFVIP
TEAVDEFKKIIGVIQASGHYSFLNVFKLFGPRNQAPLSFPIPGWNICVDFPIKDGLGKF
VSELDRRVLEFGGRLYTAKDSRTTAETFHAMYPVDEWISVRRKVDPLRVFASDMA
RRLELL
```

FASTA Entry of P9WJF1

>sp|P9WJF1|DPRE1_MYCTU Decaprenylphosphoryl-beta-D-ribose oxidase

OS=Mycobacterium tuberculosis (strain ATCC 25618 / H37Rv) OX=83332 GN=dprE1

PE=1 SV=1

MLSVGATTTATRLTGWGRTAPSVANVL RTPDAEMIVKAVARVAESGGGRGAIARG
LGRSYGDNAQNGGGLVIDMTPLNTIHSIDADTKLVDIDAGVNLDQLMKAALPFGLW
VPVLPGTRQVTVGGAIACDIHGKNHHSAGSFGNHVRSMDLLTADGEIRHLTPTGEDA
ELFWATVGGNGLTGIIMRATIEMTPTSTAYFIADGDVTASLDETIALHSDGSEARYTY
SSAWFDAISAPPKLGRAAVSRGRLATVEQLPAKLRSEPLKFDAPQLLTPDVFPNGLA
NKYTFGPIGELWYRKSGTYRGKVQNL TQFYHPLDMFGEWNRAYGPAGFLQYQFVIP
TEAVDEFKKIIGVIQASGHYSFLNVFKLFGPRNQAPLSFPIPGWNICVDFPIKDGLGKF
VSELDRRVLEFGGRLYTAKDSRTTAETFHAMYP RVDEWISVRRKVDPLRVFASDMA
RRLELL

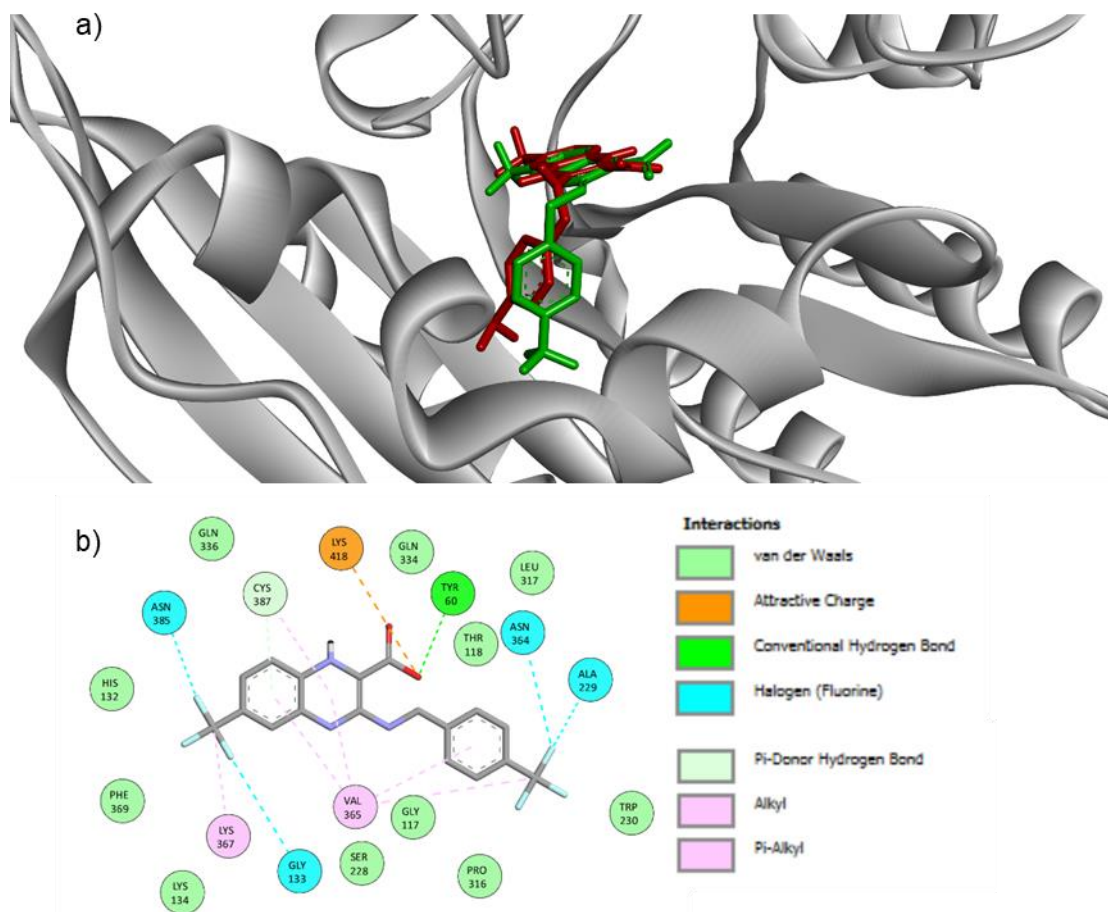


Figure S1 a) Comparison of the crystal structure and the predicted pose of Y22 in DpRE1.

Protein is rendered as a ribbon and coloured silver. In the crystal pose of Y22 is coloured green and the docked pose of Y22 coloured red) b) 2D interaction plot of the docked pose of Y22 with DpRE1.

Results and Discussion

Wild-Type: The top three ligand molecules, ZINC5, ZINC8 and PTZ were observed in the catalytic groove of DpRE1. Hydrogen interactions are formed by Lys418 residue with the oxygen atom and Tyr415 residue with the fluorine atom for all the three ligand molecules. However, differences have been observed in molecular interactions of the active site residues of DpRE1. The ZINC5 ligand shows hydrogen bonding interactions with Thr118, His132 and Gln336 residues with the oxygen atoms. The residues Leu317, Leu363, Val365, Ile131, Cys129 and Ala417 show alkyl and pi-alkyl interactions with the ZINC5 molecule. Tyr60 forms pi-stacking interactions with the aromatic ring of ZINC5, whereas it forms hydrogen interactions with the oxygen atom of PTZ (Figure S2). The residues Gln334 and His132 show

hydrogen bonding interactions with the oxygen atoms and Arg58 residue forms halogen interaction with the fluorine atom of ZINC8 ligand molecule. Cys129 and Ala417 residues form pi-alkyl and alkyl interactions with ZINC8 ligand molecule. Tyr415 residue forms pi-pi T-shaped interactions with the aromatic ring of ZINC8. The NH₂ group in the ZINC8 ligand molecule makes hydrogen bonding interactions with His132. With respect to the PTZ ligand, hydrogen bonding interactions are formed by the Gly117 and Lys418 residues with the oxygen atoms and Tyr415 with the fluorine atom. Also, the residues Arg58, Ala417, Val121, Cys129, Ile131, Leu363, Val365 and Cys387 form alkyl and pi-alkyl interactions with the PTZ ligand) Overall, the excellent interaction network of DprE1 residues had been observed with ZINC5 as compared to the ZINC8 and PTZ ligand molecules.

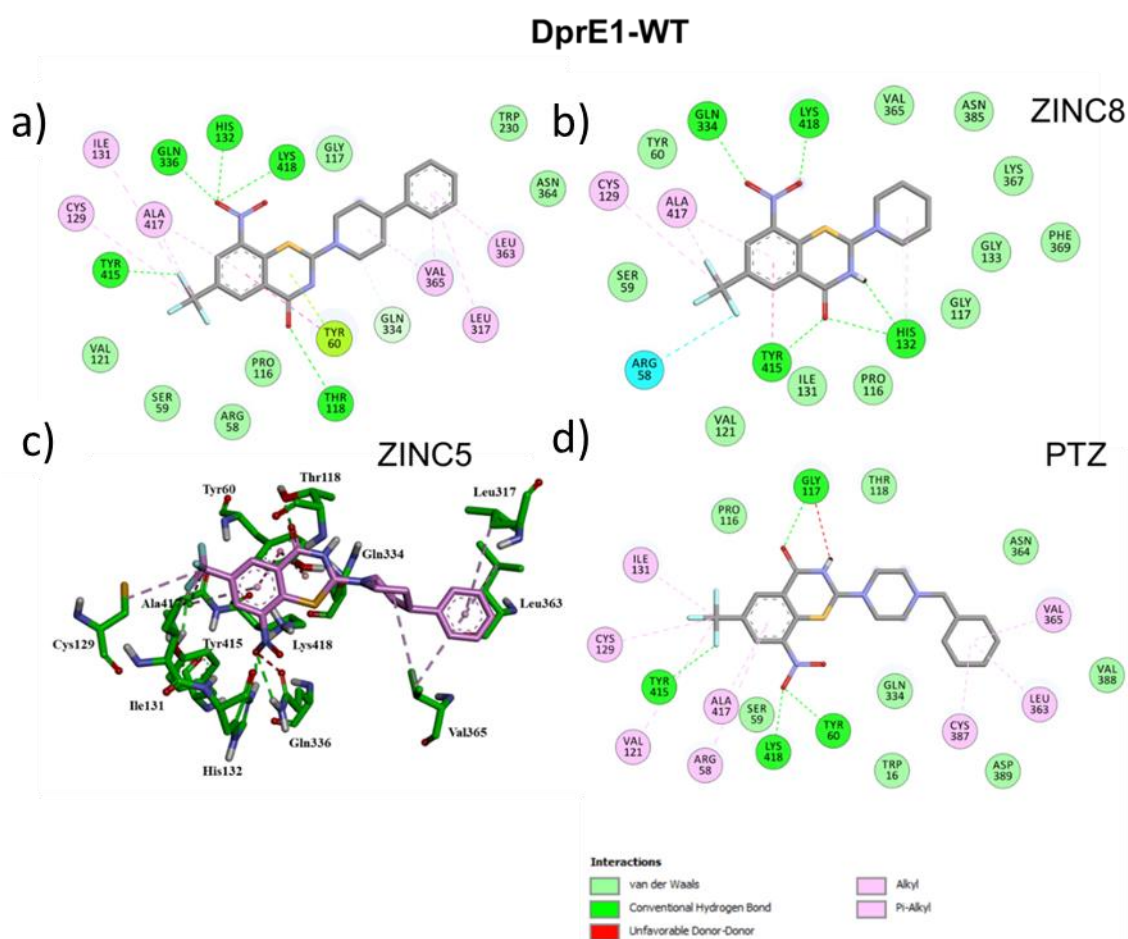


Figure S2 Representation of top 3 ligands interacting with Wild-type DprE1 (DprE1-WT)

active site a) ZINC 5, b) ZINC8, c) ZINC5 (in 3D), d) PTZ

Figure S3 Representation of top 3 ligands interacting with MutC387A active site a) ZINC 5,
c) ZINC5 (in 3D), b) ZINC28, d) ZINC41

Cys387-Gly387: The interactions of ZINC5, ZINC28 and ZINC17 ligands with the mutated model C387G. The residues Ile131, Pro116, Ala417 show alkyl and pi-alkyl interactions in all the three ligands. Despite a few similarities, there are many differences observed in the interactions formed by other residues with these three ligand molecules. The fluorine atom of ZINC5 makes halogen interactions with the residues Asn385, Ile386, Phe366 and Val365 (Figure S4). The residues Lys367 and Arg58 also show alkyl and pi-alkyl interactions with the ZINC5 ligand molecule. Also, Val121 shows pi-sigma interactions with the aromatic ring of the ZINC5 ligand (Figure S4). The NH₂ group of ZINC5 and ZINC28 makes H-bonding interaction with His132 residue. Lys367, Phe369, Val121 and Tyr415 residues show alkyl and pi-alkyl interactions with the ZINC28 ligand molecule. Hydrogen bonding interactions are exhibited by the Tyr60 and Lys 418 residues with the oxygen atom, and Cys129 residue with the fluorine atom of the ZINC28 ligand molecule. Whereas Tyr415 residue displays pi-sulfur interaction with the sulfur atom and Gly125 residue displays halogen interactions with the fluorine atom of ZINC28 ligand molecule. ZINC17 ligand has a fewer number of interactions viz. Lys418 shows pi-cation activity with the aromatic rings of the ligand; and the amino acids Lys367, Phe369, Ile131, Pro116 and Ala417 experience alkyl and pi-alkyl interactions.

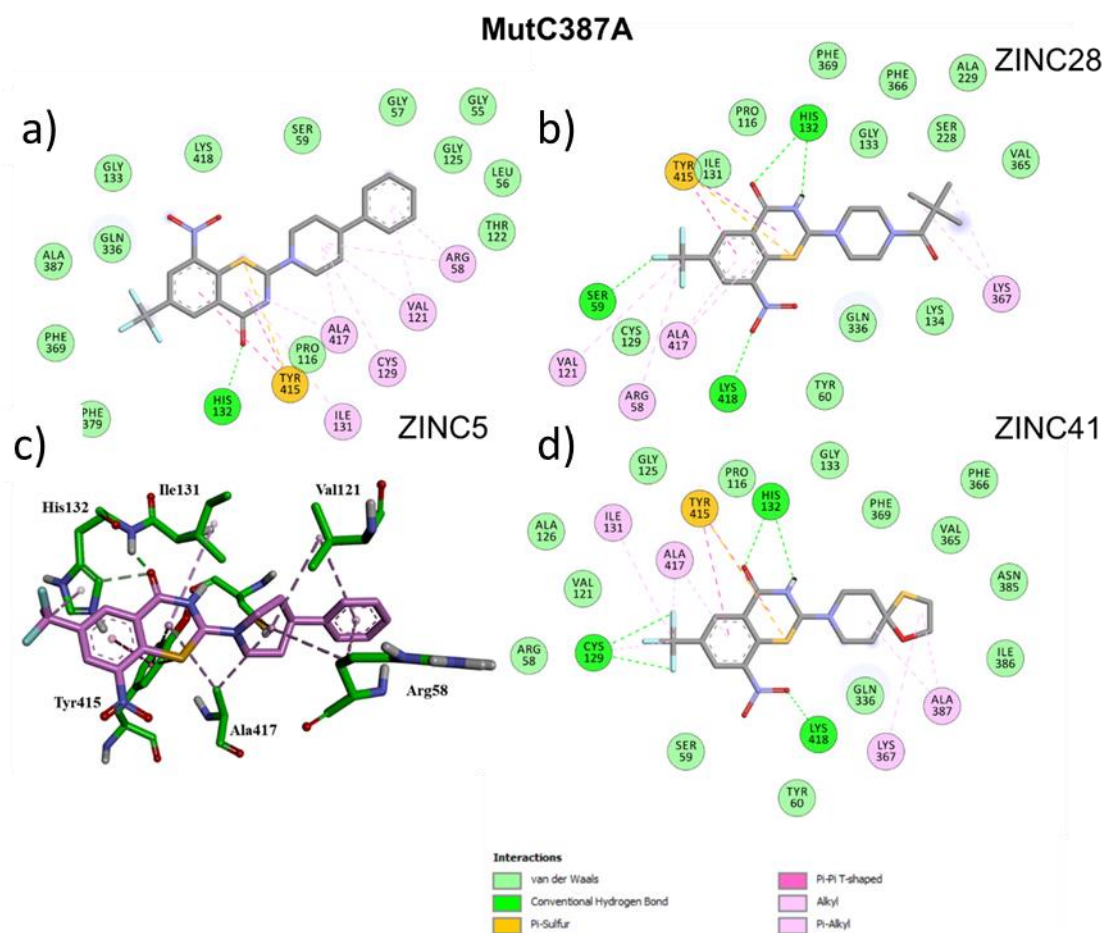


Figure S4 Representation of top 3 ligands interacting with MutC387G active site a) ZINC 5, b) ZINC28, c) ZINC5 (in 3D), d) ZINC17

Cys387-Asn387: The top three ligands interacting with C387N mutant model are ZINC10, ZINC36 and BTZ043. Ala417 interacts with all the three ligand molecules via alkyl and pi-alkyl interactions, whereas Lys418 and His132 do so via H-bonding with the oxygen atoms. H-bonding interactions are depicted in the ZINC10 ligand by the residue Gln336 with the oxygen atom, by the Lys418 residue with the sulfur atom and by the Tyr415 residue with the NH₂ group. Additionally, Tyr415 makes pi-sulfur interactions with the sulfur atom, and alkyl and pi-alkyl interactions with the ZINC10 ligand molecule. Gly133 and His132 make halogen interactions with the fluorine atoms of the ZINC10 ligand) Additionally, ZINC10 shows alkyl and pi-alkyl interactions with Ile131, Val121, Cys129 and Arg58 (Figure S5). The sulfur atom of ZINC36 interacts with Ser228 via pi-sulfur bond, and the accompanying

carbon atom shows pi-alkyl interaction with Lys367. Pro116 exhibit alkyl and pi-alkyl interactions and Tyr415 exhibits pi-pi T-shaped interactions with carbon ring structures of the ZINC36 ligand) Cys129 shows hydrogen bonding interaction and Arg58 forms halogen bonding interactions with the fluorine atom for the ZINC36 ligand) BTZ043 shows alkyl and pi-alkyl interactions with Pro116, Ile131, Tyr415 and Lys367 residues. Val365, Asn385 and Phe366 show halogen interactions with the fluorine atoms of BTZ043 ligand molecule. Cys129 makes hydrogen bonding interactions with the oxygen atom of BTZ043.

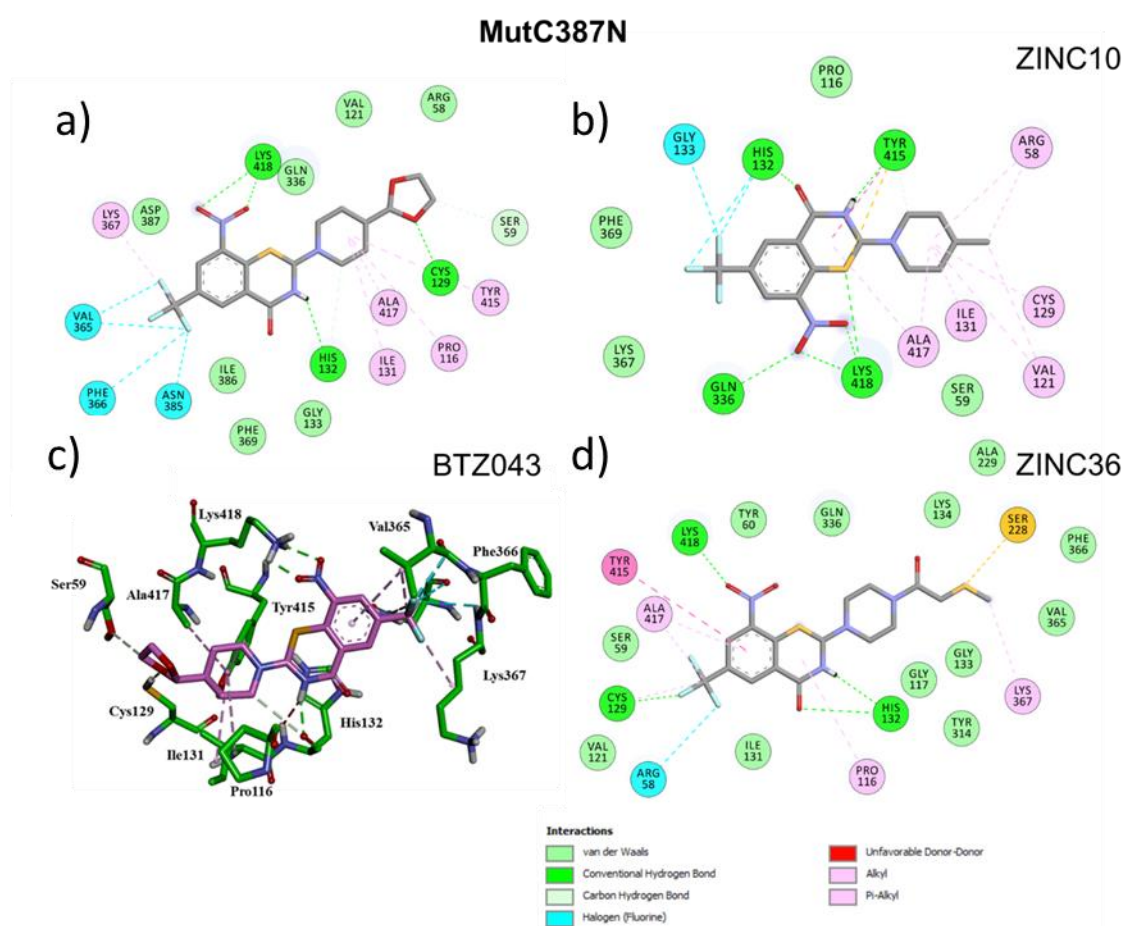


Figure S5 Representation of top 3 ligands interacting with MutC387N active site a) BTZ043
5, b) ZINC10, c) BTZ043 (in 3D), d) ZINC36

Cys387-Ser387: ZINC36, ZINC5 and PBTZ169 are the top three ligands that show interaction with MutC387S model. Tyr415 shows pi-sulfur interaction with the sulfur atom of all the three ligands ZINC36, ZINC5 and PBTZ169, it also shows pi-pi T-shaped interactions

with the aromatic rings of ZINC36 and PBTZ169, and pi-Sigma interactions with the aromatic rings of ZINC5 and PBTZ169. The oxygen atom of all three ligands ZINC36, ZINC5 and PBTZ169 makes H-bonding interactions with Lys418. The His132 residue makes H-bonding interactions with the NH₂ group of all three ligands ZINC36, ZINC5 and PBTZ169. Additionally, many other residues show varied type of interactions with each of these three ligand molecules. The fluorine atom exhibits H-bonding interactions with Ser59 and Cys129 residues of ZINC36, Ser387 residue of ZINC5 and Cys129 residue of PBTZ169 (Figure S6). The residues Val121, Arg58 and Cys129 show alkyl and pi-alkyl interactions with ZINC36. Also, Ala417 and Pro116 show alkyl and pi-alkyl interactions with the aromatic ring of ZINC36. The fluorine atom of ZINC5 also makes halogen interactions with residues Asn385 and Val365, however, no halogen interactions are shown in ZINC36 and PBTZ169. The residues Val365, His132, Ala417, Ile131, Pro116, and Cys129 interact by alkyl and pi-alkyl interactions with ZINC5. Also, Val121 and Arg58 show alkyl and pi-alkyl interactions and Cys129 shows pi-sulfur interaction with the aromatic ring of ZINC5.

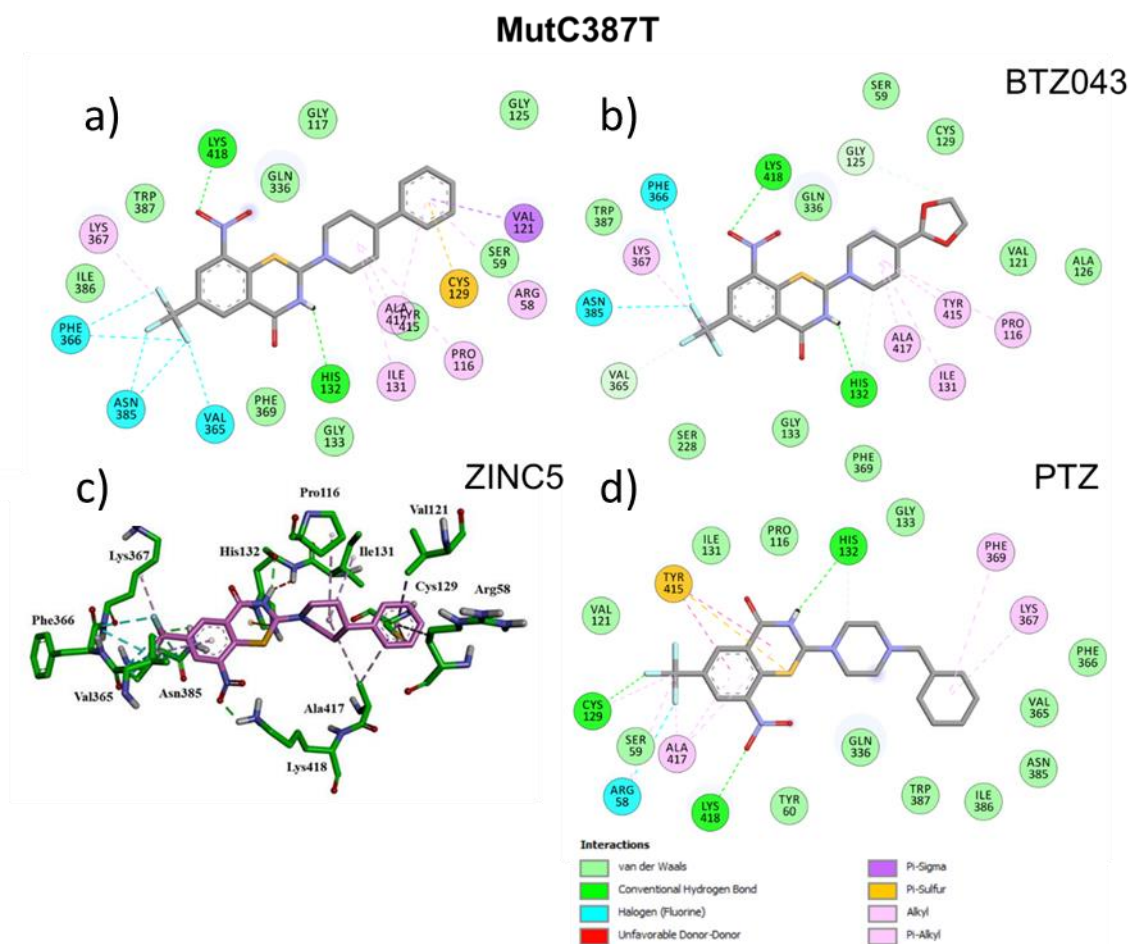


Figure S6 Representation of top 3 ligands interacting with MutC387S active site a) ZINC 5, b) ZINC36, c) ZINC5 (in 3D), d) PBTZ169

Cys387-Thr387: BTZ043, PBTZ169 and ZINC5 are the top three ligands that show interaction with C387T mutant model. Lys418 residue shows H-bonding interaction with the oxygen atom and His132 residue makes H-bonding interactions with the NH₂ group of all the three ligands BTZ043, PBTZ169 and ZINC5. There are multiple variations found in the types of bonding and interactions for many residues with each of the three ligand molecules. Halogen interactions are formed by the fluorine atom of the ligand BTZ043 with residues Phe366 and Asn385; the ligand PBTZ169 with residues Arg58; and the ligand ZINC5 with residues Phe366 and Asn385. The residues Lys367, Ala417, Ile131, Tyr415 and Pro116 extend alkyl and pi-alkyl interactions towards BTZ043 ligand (Figure S7). Tyr415 residue shows pi-sulfur interaction with the sulfur atom, and pi-pi T-shaped interaction with the

aromatic rings of PBTZ169. Cys129 residue shows H-bonding interaction with the fluorine atom of PBTZ169. The residues Cys129, Arg58, Ala417, Lys367 and Phe369 show alkyl and pi-alkyl interactions with PBTZ169. Val365, Asn385 and Phe366 forms halogen bonding with fluorine atoms of ZINC5. The residues Lys367, Ile131, Pro116 and Ala417 show alkyl and pi-alkyl interactions with ZINC5. Also, Val121 show pi-sigma interaction, Arg58 and Ala417 show alkyl and pi-alkyl interaction, and Cys129 shows pi-sulfur interaction with the aromatic rings ZINC5.

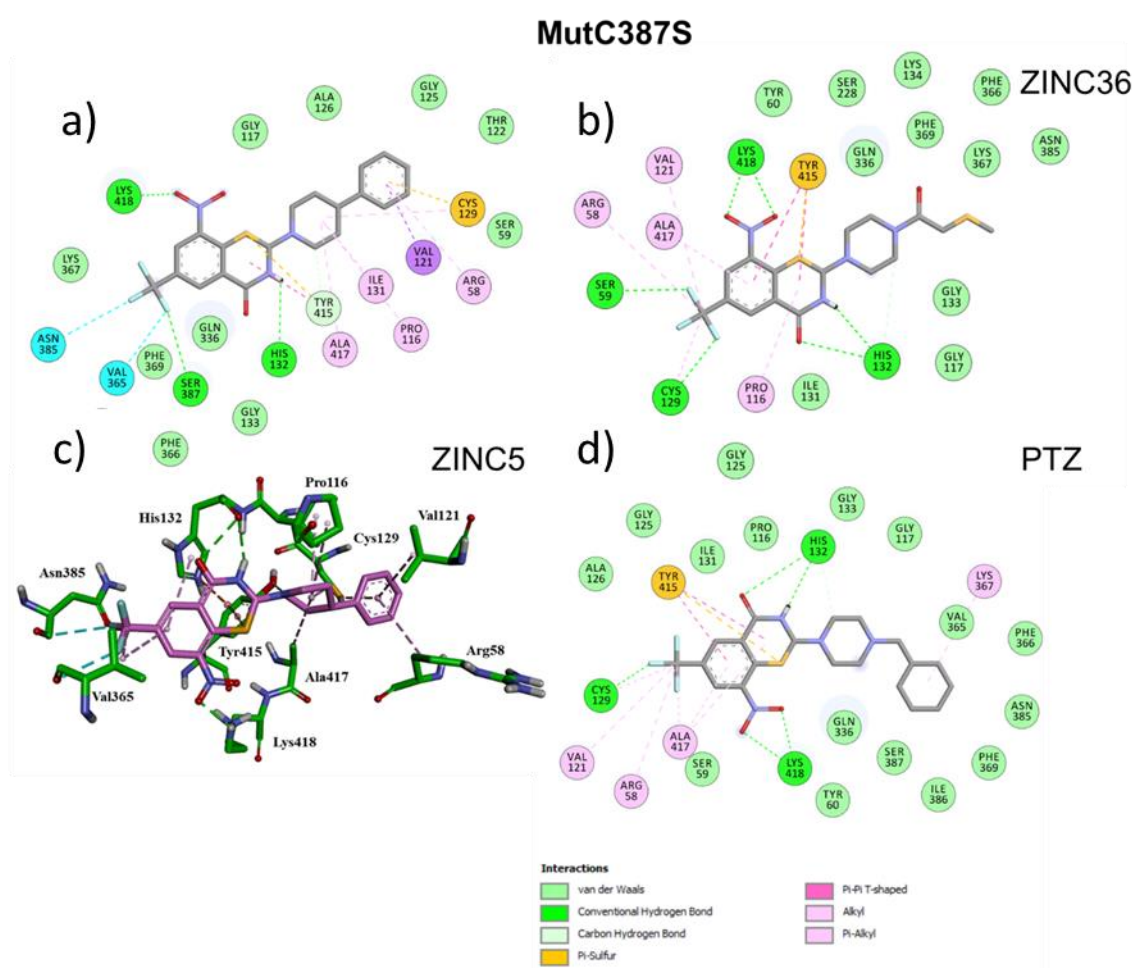


Figure S7 Representation of top 3 ligands interacting with MutC387T active site a) ZINC 5, b) BTZ043, c) ZINC5 (in 3D), d) PBTZ169

Leu368-Pro368: ZINC5, ZINC28 and PBTZ169 are the top three ligands that show interaction with MutL368P model. Ile131 shows alkyl and pi-alkyl interactions with all three ligands ZINC5, ZINC28 and PBTZ169. Other residues show differences in the types of

interactions with each ligand) The fluorine atom of ZINC5 makes Halogen interactions with Gln336 residue. The oxygen atom of ZINC5 makes H-bonding interactions with His132 residues (Figure S8). The residues Ala417, Arg58, Val121 and Cys129 show alkyl and pi-alkyl interactions with the ZINC5 ligand molecule. Also, Val121 and Arg58 show alkyl and pi-alkyl interaction, and Cys129 show pi-sulfur interaction with the aromatic rings of ZINC5. The Try415 residue shows pi-pi T-shaped interaction with both the ligands ZINC5 and PBTZ169. Lys418 and Tyr60 residues show H-bonding interactions with the oxygen atom of both ZINC28 and PBTZ169, whereas His132 residue shows H-bonding interactions with the oxygen atom of only ZINC28 ligand) His132 residue also shows H-bonding interaction with the NH₂ group of both ZINC28 and PBTZ169. The fluorine atom of both the ligands ZINC28 and PBTZ169 makes Halogen interactions with Gly125 residue, and H-bonding interactions with Ser59 and Cys129 residues. The Try415 residue shows pi-sulfur interaction with the sulfur atom of ZINC28 and PBTZ169. The residues Ala417, Ile131, Val121, Lys367 and Phe369 show alkyl and pi-alkyl interactions with ZINC28 ligand) The Ala417 residue shows pi-sigma interactions with the aromatic ring of only PBTZ169 ligand) The residues Ile131, Pro116, Val121, Arg58 and Lys367 show alkyl and pi-alkyl interactions with PBTZ169 ligand.

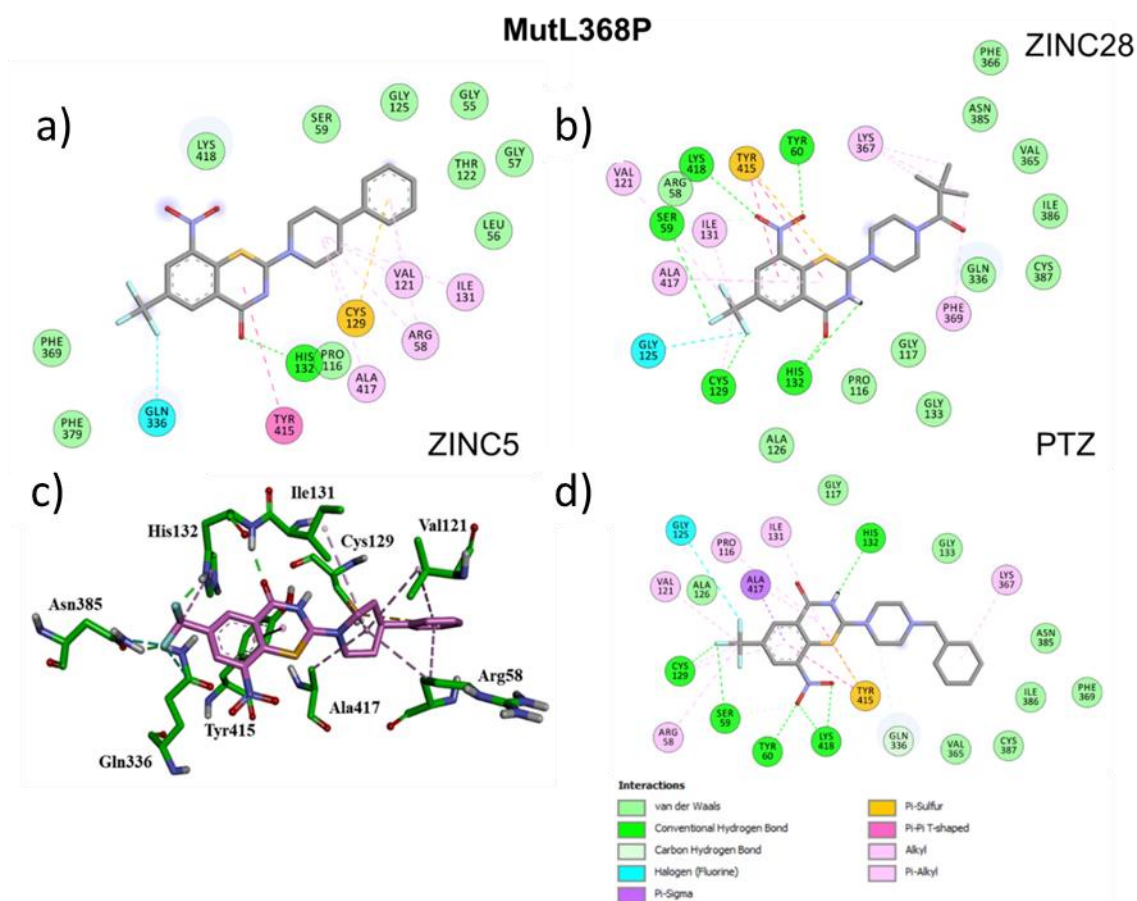


Figure S8 Representation of top 3 ligands interacting with MutL368P active site a) ZINC 5, b) ZINC28, c) ZINC5 (in 3D), d) PBTZ169

Gly17-Cys17: Top three ligands ZINC10, ZINC39 and ZINC5 show interaction with MutG17C model. Tyr415 shows pi-pi T-shaped interaction with the aromatic ring of all three ligands ZINC10, ZINC39 and ZINC5. However, there are several differences observed for interaction of other residues with each ligand) His132 residue shows Halogen interactions with the fluorine atom and H-bonding interactions with the oxygen atom of ZINC10, whereas it shows Halogen interactions with NH₂ group of ZINC39 and makes H-bonding interaction with the NH₂ group of ZINC5. Gly133 residue also shows Halogen interactions with the fluorine atom of ZINC10 (Figure S9). The residues Phe369, Cys129, Ile131, Val121, Arg58 and Ala417 show alkyl and pi-alkyl interactions with ZINC10. The oxygen atom of both ZINC39 and ZINC5 makes H-bonding interactions with Lys418 residue. The Fluorine atom

makes alkyl and pi-alkyl interactions with Pro116 and Ile131 residues of ZINC39. Also, Ala417, Val121 and Lys367 residues show alkyl and pi-alkyl interactions with ZINC39. The fluorine atom of ZINC5 makes Halogen interactions with residues Asn385 and Val365. The residues Phe369, Lys367, Ile131, Pro116 and Ala417 show alkyl and pi-alkyl interactions with ZINC5. Also, Val121 show pi-sigma interaction, Arg58 show alkyl and pi-alkyl interaction, and Cys129 show pi-sulfur interaction with the aromatic rings of ZINC5.

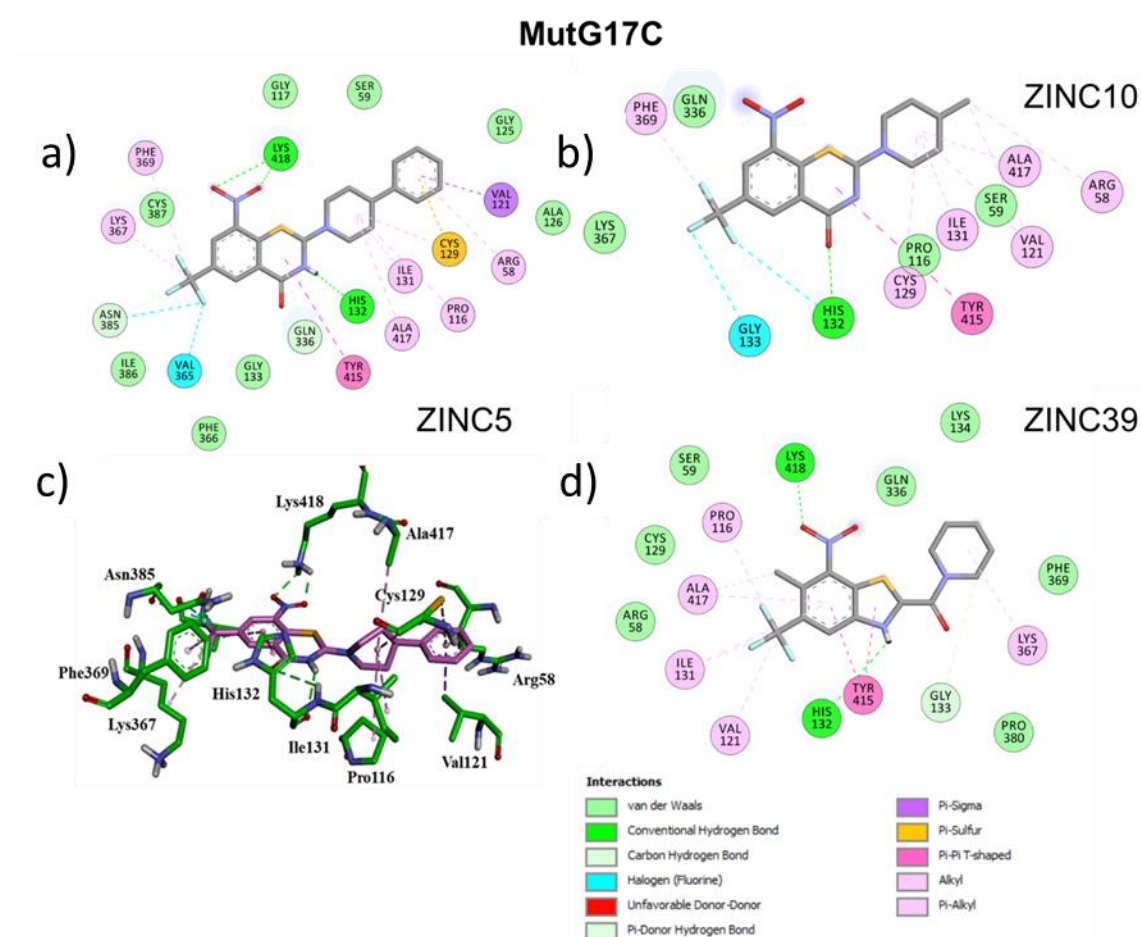


Figure S9 Representation of top 3 ligands interacting with MutG17C active site a) ZINC 5, b) ZINC10, c) ZINC5 (in 3D), d) ZINC39

Mut-All (Gly17Cys, Leu368Pro, Cys387Ala): The top three ligands which bind the Mut-All model are ZINC5, ZINC7 and ZINC17. Only Val121 shows alkyl interactions common in all the three ligands. Arg58, Ala417 and Pro116 react with the carbon rings of ZINC5 via alkyl and pi-alkyl interactions Cys129 shows pi-sulfur and pi-alkyl interactions with ZINC5

(Figure S10). Along with alkyl and pi-alkyl reactions and pi-sigma reactions with the ligands ZINC5 and ZINC7 respectively, the Tyr415 residue also exhibits pi-sulfur interactions with the sulfur atom of both these ligand) His132 represents Hydrogen bonding interactions with the oxygen atom of ZINC5 and ZINC7 ligands, whereas Lys 418 represents the same only with ZINC5 ligand) Also, His132 makes halogen interactions with the fluorine atom, and forms alkyl and pi-alkyl interactions with the carbon atoms of ZINC5 ligand) Additionally, Gln336 and Asn385 residues exhibit halogen interactions with the fluorine atoms of ZINC5 ligand, whereas Gln336 forms hydrogen bonding interactions with the fluorine atom of ZINC7 ligand) Try415 also forms hydrogen bonding interactions with the NH₂ group of the ZINC7 ligand) ZINC7 interacts with Ile131, Arg58, Cys129, Ala417 and Phe369 residues via pi-alkyl and alkyl interactions. With respect to the ZINC17 ligand, alkyl and pi-alkyl interactions are formed by Ala387, Lys367, Phe369, Ile131 and Pro116 residues. In ZINC17, H-bonding interactions are formed with the oxygen atom only by Thr118 residue. Also, only Lys418 residue had been observed to form pi-cation interactions with the ZINC17 ligand.

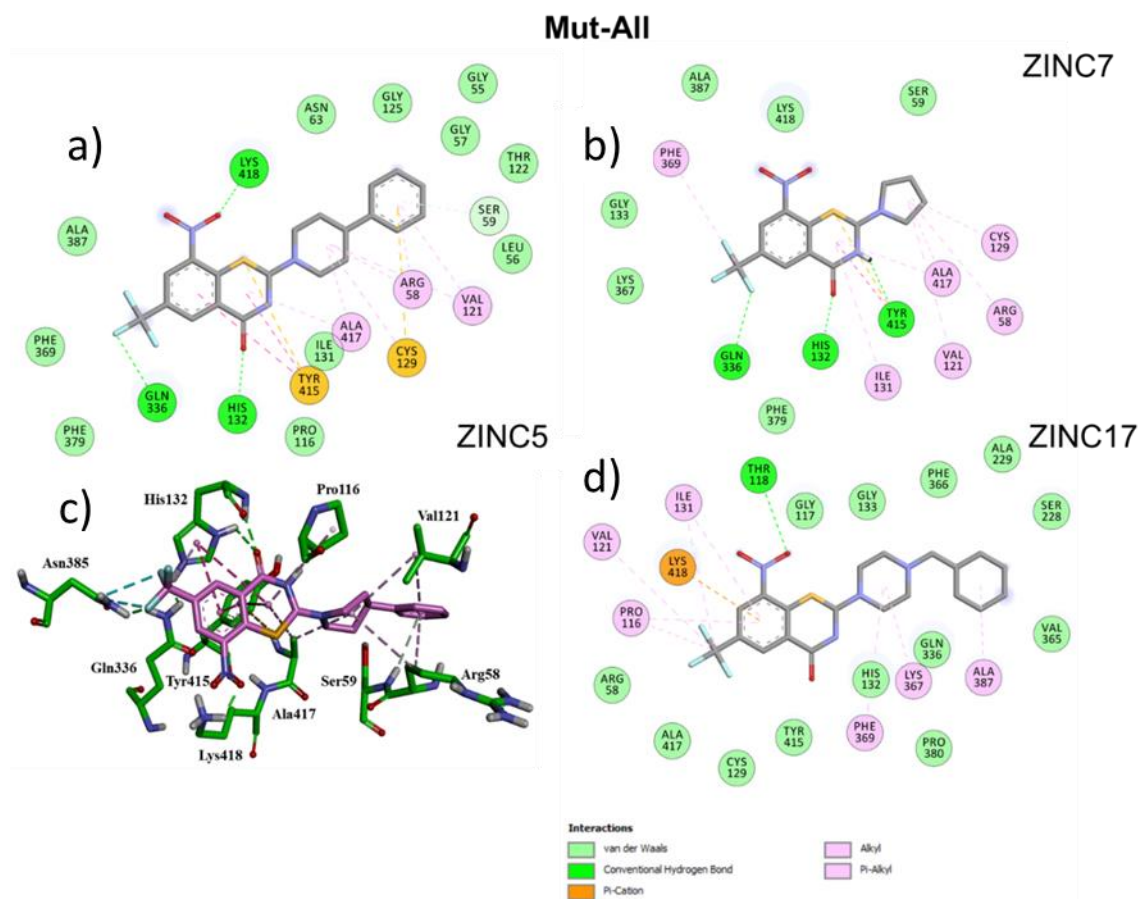


Figure S10 Representation of top 3 ligands interacting with Mut-All active site a) ZINC 5, b) ZINC7, c) ZINC5 (in 3D), d) ZINC17

Table S1 The ZINC ID replaced with shorter names for convenience.

Original ZINC ID	Nomenclature used in Manuscript
ZINC000141433347	PTZ1
ZINC000043208590	ZINC1
ZINC000070466414	ZINC2
ZINC000095572721	ZINC3
ZINC000095572794	ZINC4
ZINC000095577489	ZINC5
ZINC000095577552	ZINC6
ZINC000096910801	ZINC7
ZINC000096910802	ZINC8
ZINC000096910803	ZINC9
ZINC000096910804	ZINC10
ZINC000096910805	ZINC11
ZINC000096910807	ZINC12
ZINC000096910808	ZINC13
ZINC000103248023	ZINC14
ZINC000103248024	ZINC15
ZINC000103248972	ZINC16
ZINC000110473906	ZINC17
ZINC000141433347	ZINC18
ZINC000141440904	ZINC19
ZINC000169351315	ZINC20
ZINC000169351317	ZINC21
ZINC000169351318	ZINC22
ZINC000169353746	ZINC23
ZINC000169353748	ZINC24
ZINC000169353749	ZINC25
ZINC000210462992	ZINC26
ZINC000210463040	ZINC27
ZINC000210463087	ZINC28

ZINC000210463131	ZINC29
ZINC000210463176	ZINC30
ZINC000210466905	ZINC31
ZINC000210466998	ZINC32
ZINC000223193481	ZINC33
ZINC000263620243	ZINC34
ZINC000299856973	ZINC35
ZINC000299858082	ZINC36
ZINC000299859114	ZINC37
ZINC000299864522	ZINC38
ZINC000299865195	ZINC39
ZINC000653781805	ZINC40
ZINC000653795167	ZINC41